PERGAMON

International Journal of Heat and Mass Transfer 44 (2001) 3147–3153

International Journal of HEAT and MASS TRANSFER

www.elsevier.com/locate/ijhmt

The liquid temperature in diffusion controlled vapor condensation: analysis and experimental verification

Franz Peters *, Arne Graßmann

Strömungslehre FB 12, Universität Essen, Schützenbahn 70, 45127 Essen, Germany

Received 29 September 1999; received in revised form 27 September 2000

Abstract

This work deals with the temperature of a liquid film that forms on a thin wire by condensation of vapor present in ambient gas at a small fraction. Based on heat and mass transfer theory in the continuum regime, it is shown that the liquid temperature is steady when the ambient state is steady while a boundary layer in-between may develop in time. An expression for the calculation of the liquid temperature is derived being valid for the geometry of the wire and two other 1-D geometries, namely a plane wall and a sphere. Experiments are carried out with a cylindrical thin wire, the electrical resistance of which was measured in order to obtain the liquid temperature. Results are provided for condensing alcohol and water films showing good agreement with the calculated temperature.

Keywords: Condensation; Heat transfer; Thin films

1. Introduction

We consider a resting inert carrier gas containing a relatively small fraction of a condensible vapor. The vapor/carrier mixture is in non-equilibrium contact with the liquid phase of the vapor substance so that either condensation or evaporation takes place. In view of our experiments, we refer to condensation, in what follows, knowing that evaporation is just the reversed process described by the same set of equations. The liquid mass has a small volume to area ratio and it is isolated or insulated in a way that it can exchange mass and heat only with the surrounding gas. Fig. 1 shows three cases considered in the present study. The first case presents a thin liquid film on a perfectly insulated plane wall of infinite extension or a very thin foil with liquid films on both sides (not shown). In the second case, we consider a very small cylinder (e.g. a wire of 5 μm) coated with a liquid film. The third case corresponds to either a small liquid coated sphere or a small droplet. The early stage of condensation is meant where the film is very thin and not yet subject to disturbances and gravity. In all cases mass and heat transfer is in the continuum regime which means in cases two and three that the mean free path of the gas molecules is small compared to the diameter.

In each case the vapor diffuses through the carrier gas towards the liquid surface from where the latent heat of condensation propagates back into the gas. Obviously, to maintain this process, the liquid temperature T_ℓ has to be above the ambient temperature T_∞, while the ambient pressure p_∞^{v} stays above the vapor pressure at the liquid surface. In condensation modeling, it has always been a viable assumption to equate the surface pressure with the equilibrium vapor pressure p_{e} corresponding to T_ℓ despite the presence of a driving non-equilibrium. Therefore, the vapor is in equilibrium at the liquid surface and supersaturated in the ambient state at the ratio given by

$$S = p_\infty^{\mathrm{v}}/p_{\mathrm{e}}(T_\infty). \tag{1}$$

The total pressure p_∞ is uniform throughout the transfer region as there is no bulk flow. The liquid temperature T_ℓ is the topic of this work, analytically and experimentally. Dealing with the transfer equations, we observed two remarkable properties of T_ℓ. Firstly, T_ℓ is the same in the

* Corresponding author. Tel.: +49-02-01-183-20-61; fax: +49-02-01-183-39-45.

E-mail address: franz.peters@uni-essen.de (F. Peters).

0017-9310/01/$ - see front matter
PII: S0017-9310(00)00344-6

Nomenclature

α	thermal diffusivity
c	vapor concentration (vapor density/total density)
c_p	specific heat at constant pressure
D	diffusion coefficient
$\vec{m}$	mass flux density
k	heat conductivity
L	latent heat
Le	Lewis number (α/D)
M	molar mass
n	case parameter, defined in Fig. 1
p	pressure
$\vec{q}$	heat flux density
R	specific gas constant
r	radius
$\bar{r}$	normalized radius
S	supersaturation, defined in Eq. (1)
T	temperature
t	time
τ	normalized time
w	velocity
ρ	density

Indices

ℓ	liquid
∞	ambient state
v	vapor
e	equilibrium
$*$	steady liquid temperature
0	wire

three cases of Fig. 1 and secondly, T_ℓ takes a steady-state value, independent of the temporal development of the thermal boundary layer. In the second part, we demonstrate how to measure this temperature in the case of a film coated wire. Case two lends itself to do this while the other two cases are very difficult. In case one, perfect insulation of the film against the wall is required which is difficult or impossible. In case three, the spheres are too small for sensors to be used. Optical methods offer an indirect way by measuring the refractive index which is a unique function of temperature. Mie-scattering or rainbow techniques [1] have been tried but are not yet established. As a result, experimental information on the droplet temperature is scarce. The demand for this temperature, on the other hand, is substantial because small droplets play a crucial role in dispersed systems with phase change like clouds, spray combustion and others. We cannot measure the droplet temperature either but we can do so in the cylinder case.

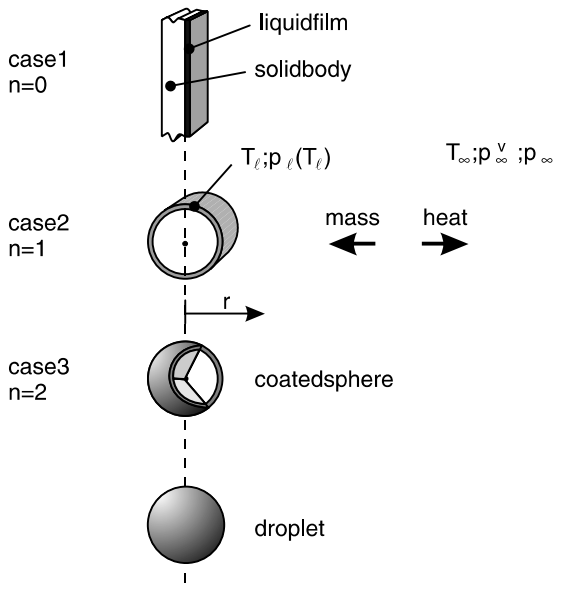

Fig. 1. Three geometrically different yet physically similar condensation situations.

We take advantage of the very small heat capacity of 5 μm tungsten wire as used for hot wire anemometry. Such a wire with a high aspect ratio ($\approx 10^4$) cools with a rapidly expanding gas from an initial to a new state of lower temperature and pressure. There, a vapor contained in the gas condenses onto the wire as a film. Film and wire temperature are equal and measurable through the electrical resistance of the wire. The temperature information extracted from this experiment is compared with the analytical result and is found to be in good agreement. Since the analytical result is equal in all three cases, a successful wire experiment enhances the confidence in the droplet temperature.

2. Analysis of the liquid temperature

Fig. 2 models the condensation process in the p–T phase diagram of the condensing vapor. The equilibrium vapor pressure curve $p_e(T)$ separates the liquid regime (left) from the vapor regime (right). A vapor/gas sample is prepared in the initial state about the thin wire. Then, by a quick isentropic expansion, gas and wire attain the temperature T_∞. The vapor pressure is now p^v_∞ which is above the equilibrium vapor pressure corresponding to T_∞. According to Eq. (1), the vapor is supersaturated and begins to condense onto the wire. Latent heat of condensation is released which can only be transferred away from the film by an increasing liquid temperature. As condensation at the liquid takes place at equilibrium,

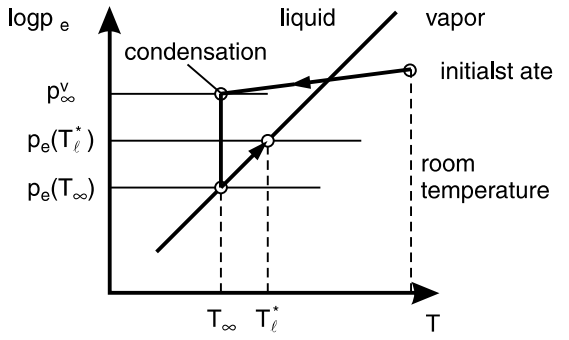

Fig. 2. The condensation situation in the log (p)–T phase diagram.

the liquid temperature moves up the coexistency curve. While the increasing temperature enhances heat transfer, at the same time it reduces the driving pressure difference. As the latter must not vanish since condensation must go on, the two effects will balance at a final T^*_ℓ. This happens in a very short time as the heat capacity of wire and film is small and the latent heat is large.

It is an important result that T^*_ℓ attains a steady value when the ambient conditions are fixed. Yet, it raises the question what T^*_ℓ depends on and how it can be calculated.

We begin with the general formulas for the local heat and mass flux densities $\vec{q}$ and $\vec{m}$:

$$\vec{q} = -k\,\mathrm{grad}(T), \tag{2}$$

$$\vec{m} = -\rho D\,\mathrm{grad}(c), \tag{3}$$

where ρ is the total density, k the heat conductivity and D is the diffusion coefficient. The concentration c is defined as the ratio of vapor and total density or expressed in pressures involving the equation of state for an ideal gas

$$c = \frac{R}{R^v}\frac{p^v}{p_\infty}. \tag{4}$$

In general, the gas constant R of the mixture varies along the path of diffusion which, however, may be ignored when the concentration gradient is moderate. Balancing heat and mass flux at the liquid surface after T^*_ℓ has been reached yields for the 1-D geometries of Fig. 1,

$$\frac{L\rho DR}{R^v p_\infty}\frac{\partial p^v}{\partial r} = k\left(-\frac{\partial T}{\partial r}\right), \tag{5}$$

where the left side represents the diffusive mass flux density multiplied by the latent heat L and the right side represents the heat flux density. (Here we have already left out the effects of convective transport. The reasons follow further down.) We now show that similarity exists between temperature and pressure and that this similarity solves Eq. (5) for T^*_ℓ.

The fundamental diffusion equations for temperature T and mass concentration c are [2]

$$\rho c_p\frac{\partial T}{\partial t} + \rho c_p \vec{w}\ \mathrm{grad}(T) = -\mathrm{div}(\vec{q}), \tag{6}$$

$$\rho\frac{\partial c}{\partial t} + \rho\vec{w}\ \mathrm{grad}(c) = -\mathrm{div}(\vec{m}). \tag{7}$$

The second term in Eqs. (6) and (7) is zero ($w = 0$) when diffusive mass fluxes are balanced so that there is no net flow. In our application the diffusive vapor flux is not balanced because the carrier gas is stagnant due to the zero velocity boundary condition at the liquid surface. The effective velocity $\vec{w}$ is then $\vec{w} = \vec{m}/\rho$. This term is often referred to as Stefan flow. Reducing to 1-D equations in r-direction we then have

$$\frac{\partial T}{\partial t} = \alpha\frac{\partial^2 T}{\partial r^2} + \frac{\alpha}{r}\frac{\partial T}{\partial r}\left(n + \frac{D}{\alpha}r\frac{\partial c}{\partial r}\right), \tag{8}$$

$$\frac{\partial c}{\partial t} = D\frac{\partial^2 c}{\partial r^2} + \frac{D}{r}\frac{\partial c}{\partial r}\left(n + r\frac{\partial c}{\partial r}\right). \tag{9}$$

The Stefan flow terms appear in the brackets and are additive to the parameter n corresponding to the cases of Fig. 1. In view of the experiments that we have conducted (cylinder $n = 1$), the question arises of what magnitude the Stefan terms are in comparison with n. With Eq. (3), we note that $r(\partial c/\partial r)$ is proportional to the time dependent mass flux which is greatest at the surface when condensation starts. Therefore, $r(\partial c/\partial r)$ should be estimated at the surface

$$r\frac{\partial c}{\partial r} = \frac{R}{R^v}r\frac{\partial p^v/p_\infty}{\partial r}. \tag{10}$$

With respect to our experiments, the greatest span of p^v/p_∞ between the surface and the surroundings is of the order 0.01. Suppose we had a gradient at the surface such that this span would occur within a distance comparable to the wire size, then the Stefan term would already be down to this negligible value 0.01 (with $R/R^v \cong 1$). As this is a worst case estimation for the experimental conditions, the Stefan term may play a role at the very beginning of condensation but certainly drops to an insignificant magnitude by the time the measurements are taken. As shown in Fig. 5, the ratio $Le = \alpha/D$ called the Lewis number is of order unity. Then Eqs. (8) and (9) with Eq. (4) reduce to

$$\frac{\partial T}{\partial \tau} = \frac{\partial^2 T}{\partial \bar{r}^2} + \frac{n}{\bar{r}}\frac{\partial T}{\partial \bar{r}}, \tag{11}$$

$$\frac{\partial p^v}{\partial \tau} = \frac{\partial^2 p^v}{\partial \bar{r}^2} + \frac{n}{\bar{r}}\frac{\partial p^v}{\partial \bar{r}}, \tag{12}$$

where the radius is normalized by the wire radius r_0 and the time by

$$\tau = \alpha t_\alpha/r_0^2 = Dt_D/r_0^2. \tag{13}$$

Due to generally different coefficients α and D, this means that the temperature solution at some τ corresponds to the real time $t_\alpha = r_0^2\tau/\alpha$ and the pressure solution to the real time $t_D = r_0^2\tau/D$.

From the similarity of these two equations, it follows that the solutions for temperature and pressure as functions of τ and $\bar{r}$ are linearly dependent on each other

$$T = Ap^{\mathrm{v}} + B, \tag{14}$$

where A and B are constants inferred from the boundary conditions

$$\begin{aligned} T_\ell^* &= Ap_{\mathrm{e}}(T_\ell^*) + B, \\ T_\infty &= Ap_\infty^{\mathrm{v}} + B, \end{aligned} \tag{15}$$

so that Eq. (14) reads

$$\frac{T - T_\ell^*}{T_\ell^* - T_\infty} = \frac{p^{\mathrm{v}} - p_{\mathrm{e}}(T_\ell^*)}{p_{\mathrm{e}}(T_\ell^*) - p_\infty^{\mathrm{v}}}. \tag{16}$$

We now use this similarity relation in Eq. (5) to replace the pressure. Then we have at the liquid

$$\left[\frac{D}{\alpha}\frac{L}{c_{\mathrm{p}}}\frac{M^{\mathrm{v}}}{Mp_\infty}\frac{p_\infty^{\mathrm{v}} - p_{\mathrm{e}}(T_\ell^*)}{T_\ell^* - T_\infty} - 1\right]\frac{\partial T}{\partial r} = 0. \tag{17}$$

As the temperature gradient cannot be zero, T_ℓ^* has to be determined such that the term in brackets becomes zero. This results in the following implicit expression for T_ℓ^*:

$$Le\frac{c_{\mathrm{p}}(T_\ell^* - T_\infty)}{L}\frac{M}{M^{\mathrm{v}}}\frac{p_\infty}{p_{\mathrm{e}}(T_\infty)} + \frac{p_{\mathrm{e}}(T_\ell^*)}{p_{\mathrm{e}}(T_\infty)} = S. \tag{18}$$

Summarizing we state that after a short initial period, T_ℓ takes a steady value T_ℓ^* that depends for a given vapor on the ambient conditions (S, T_∞, p_∞) and is independent of n. For T_ℓ^* it is not necessary to know the temporal evolution of the temperature and pressure boundary layers. When these layers are to be analyzed, Eqs. (11) and (12) need to be solved taking into account the growth of the liquid surface. For further analysis, we refer to [3] and [4]. Please note that the boundary layer of a sphere approaches a steady state which is not the case for the wall and the cylinder. This leads to the often made assumption of the overall steady state in the spherical problem (e.g. [5]) although for T_ℓ^* this would not be necessary as we have shown. Certainly, it would be incorrect to derive T_ℓ^* for the wall and the cylinder on the assumption of overall steady state.

3. Experimental

A piston-expansion (pex) tube as sketched in Fig. 3 is used to subject a vapor diluted in a carrier gas to a fast isentropic expansion from an initially undersaturated to a supersaturated state where condensation occurs (see Fig. 2). We may renounce a full description of the pex-tube with reference to droplet nucleation and growth studies for which it was originally developed ([6]; other papers quoted therein). In what follows next, we describe the essential features considering the present experiments.

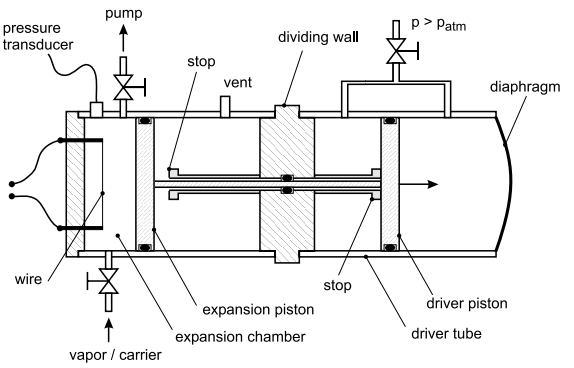

Fig. 3. Sketch of the pex-tube for the present experiments on film condensation on a thin wire.

At the left end, the tube (dia. 70 mm), the expansion piston and the end wall form the expansion chamber. The piston rod links the expansion with the driver piston operating in the driver tube. The latter extends from the dividing wall to the diaphragm at the right end. Initially, the driver piston faces equal air pressure above atmospheric on either side. When the diaphragm is broken, the pressure in front of the driver piston drops to atmospheric and the pressure difference across the piston jerks on both pistons. The expansion chamber enlarges at a dropping internal pressure creating an opposing force. By adjusting the initial pressures, all forces including mass and friction forces are balanced such that the expansion piston barely makes it to the stop where it bounces off a little bit and stops completely. The expansion pressure is measured by a dynamic pressure transducer (Kistler 6031). The total piston displacement time amounts to less than 5 ms.

The wire is obtained from a spool of wire material (tungsten) of 5 μm diameter normally used for hot wire anemometry. It is mounted 6 mm away from the end wall between two prongs 48 mm apart. The heat capacity of the wire is so small that the wire temperature follows the expansion temperature closely. At the expansion tail where the gas temperature levels off, it equilibrates with the gas temperature. When the supersaturated vapor is present and the liquid film builds up, the wire assumes the liquid temperature. Now the perfect proportionality between temperature and electrical resistance of the wire is employed (about 0.5 Ω/K). The resistance is measured by the voltage drop at a constant current of 1 mA. The calibration of the wire is explained further down along with the experimental procedure.

Two problems associated with the wire method ought to be addressed. The first is the heating of the wire by the

current of 1 mA at about 2 V corresponding to 2 mW, and the second is the heating of the wire by the prongs. Both effects are negligible. The power of the electrical heating of 2 mW fades against the power of the latent heat which is on the Watt scale. The problem with the prongs is that they do not follow the gas cooling due to their comparatively large mass. However, they release internal heat into the wire. Consequently, the wire assumes a temperature distribution instead of a uniform temperature. The analysis of this problem (for the temperature distribution, see [7]) made clear that, with the enormous aspect ratio of the wire of almost 10^4, the mean wire temperature may be off by a few tenths of a Kelvin at the most.

The experimental procedure is to be discussed along with Figs. 3 and 4. In first place, the stops are set and the initial length (e.g. 15 mm) of the expansion chamber as well as the piston travel are determined by a dial gauge to an accuracy of 1/100 mm. This way the expansion volume ratio is known. Then dry carrier gas (nitrogen with the ratio of specific heats of 1.4) is supplied to the expansion chamber at a well controlled pressure near 750 Torr (Baratron 390 HA). The initial temperature is set by electrical heating above room temperature and measured by a Pt-100. The driver tube is loaded with air to a pressure above atmospheric and the diaphragm is ruptured. Expansion pressure and wire voltage at 1 mA are monitored by a high-speed data acquisition board plugged into a personal computer. An example is reproduced in Fig. 4 where curve 1 gives the pressure. With the piston starting at time zero, the initial pressure drops rapidly. The lowest value corresponds to the piston travel, i.e. where the piston reaches the stop. (The expansion chamber is too short to show discernible wave action.) Since the pressure at this point is precisely known from the initial pressure and the volume expansion ratio, the calibration of the pressure transducer is at hand. The only restriction would be heat entering the chamber during expansion spoiling its isentropic character. We have calculated that this effect is very small in the few ms of expansion.

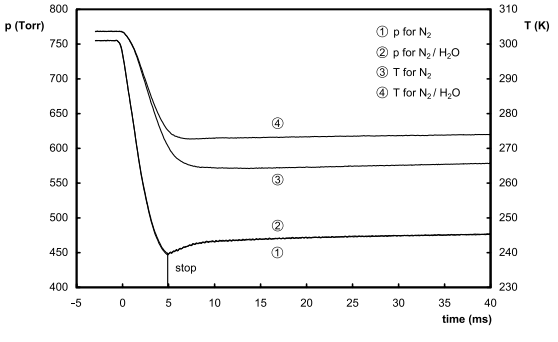

Fig. 4. Typical traces of pressure expansion and wire temperature.

After the lowest point, the pressure recovers a bit due to the bouncing piston before it levels off. Here the pressure is secured by the calibration irrespective of the heat question. We see that the corresponding wire temperature (curve 3) levels off like the pressure. We calculate the wire temperature from the pressure signal isentropically and use it to calibrate the wire (at 20 ms). Now it may be argued that heat has certainly entered the tube by that time. This is so, yet heat enters at the walls and the compression of the gas core that has not been reached by the heat is still isentropic. It just has to be calculated what the propagation velocity of the heat front is and that the wire has not been attacked by it (see [6]).

After these two calibrations, the desired vapor/gas mixture is prepared in a mixing tank (not shown) by partial pressure measurements (Baratron 390 HA) and filled into the expansion chamber. Then the expansion is repeated. The expansion pressure (curve 2) collapses exactly with the first curve demonstrating the reproducibility of the process. Curve 4 appears elevated with respect to curve 3 due to film condensation. The corresponding temperature is obtained using the previous calibration and the supersaturation (Eq. (1)) is evaluated accordingly. After this, the water vapor content is changed and the procedure is repeated. This way a sequence of isothermal data points $T_\ell^* - T_\infty$ vs S is collected.

4. Results

Experiments were conducted with *n*-propanol, ethanol and water carried in nitrogen. De-ionized water was used with a residual electrical conductivity of (3 MΩ cm)$^{-1}$ which is too low to contribute to the conductivity of the tungsten wire. Perfect wettability of the wire by the three liquids was checked by contacting a liquid surface in a dish. The question whether the wire is wetted immediately and completely when the vapor starts to deposit cannot be answered. Most likely, slight supersaturations are necessary to overcome heterogeneous nucleation barriers. Then at least evenly distributed condensation sites may be expected which grow together forming a film. With the rather high supersaturations in the experiments, the heterogeneous barrier would not be noticed.

Results are presented in Figs. 6–8. Plotted is the temperature difference between liquid and surroundings $T_\ell^* - T_\infty$ vs the supersaturation S. Each data curve refers to a certain volume expansion which produces a nominal T_∞ and p_∞ as indicated and explained above. Not all experimental runs hit T_∞ exactly. The reason is two-fold. Firstly, the initial temperature (room temperature) is not perfectly stable. Secondly, the ratio of specific heats is slightly affected due to the vapor addition. This affects T_∞ noticeably in the alcohol/nitrogen expansions while it

is negligible for water/nitrogen. The deviation from the indicated T_∞ is about ± 1 K for the alcohols and less for water.

The plotted lines represent the theory according to Eq. (18) employing the indicated T_∞ and p_∞ for each line. Following [8], the diffusion coefficient D was evaluated from the Chapman–Enskog model. With $k(T)$ found in the same book, with c_p of nitrogen and the density, the Lewis number was calculated as function of temperature. Fig. 5 shows that the temperature dependence is marginal. The Lewis number does not depend on pressure anyway. The same behavior is found for the Fuller model for $D(T)$ ([8]) except that Le takes different values. The vapor pressures of alcohols are found in [9], and the one for water is taken from [10] who extrapolate the liquid vapor pressure below the triple point. The liquid film is not expected to freeze on the present time scale. With the vapor pressures at hand, the latent heats are inferred by the Clausius–Clapeyron equation. No mixing rules are involved for the properties Le, c_p and M in Eq. (18) because the effect on T_ℓ^* is irrelevant.

Figs. 6 and 7 display the results for n-propanol and ethanol. Three curves for three different ambient states

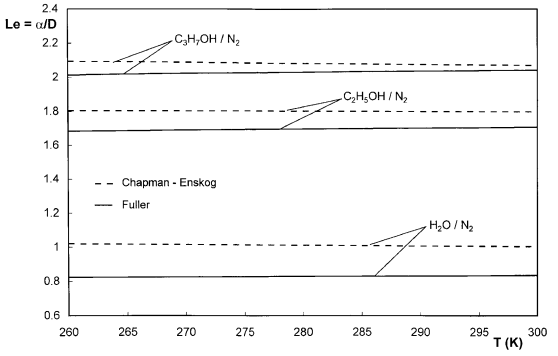

Fig. 5. The Lewis number as function of temperature for the investigated vapor/carrier systems.

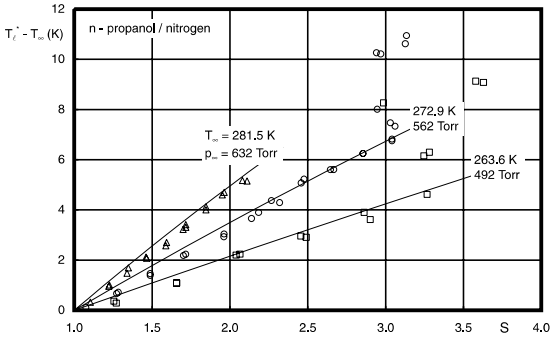

Fig. 6. Experimental results (symbols) and theory (lines) for the excess temperature of the condensing film vs the supersaturation of the ambient vapor for n-propanol in nitrogen.

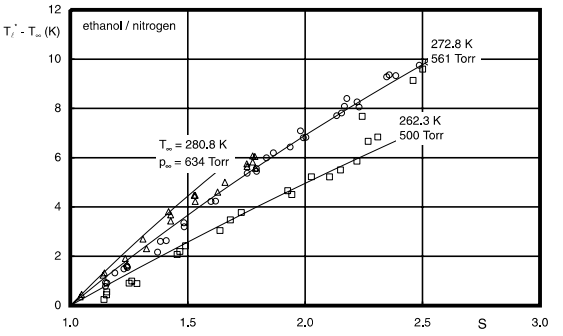

Fig. 7. Experimental results (symbols) and theory (lines) for the excess temperature of the condensing film vs the supersaturation of the ambient vapor for ethanol in nitrogen.

$(T_\infty,\ p_\infty)$ were measured for each substance (points). The maximum reached excess temperature is about 7 K with propanol and 10 K with ethanol. Supersaturations tend to be smaller for ethanol. The theoretical model of Eq. (18) predicts the variations in terms of substance, temperature, pressure and supersaturation consistently and correctly. Deviations are of the order of the experimental data scatter which lies within a Kelvin. Relative to the excess temperature, this may not be considered small. On the other hand, the resolution of a transient temperature down to a Kelvin is a remarkable result. The theoretical curves are calculated using the Chapman–Enskog model (Fig. 5). As the curves for the Fuller model come very close, they are not plotted.

Things change beyond certain limits of S where the bottom data curve for ethanol and the bottom and middle curves for propanol begin to scatter dramatically. This behavior has a perfect explanation. The supersaturated state produces homogeneous nuclei as condensation sites at a rate that depends exponentially on S. This rate was measured before [11,12]. A strong increase of the rate was found above $S = 4$ for propanol and above $S = 3$ for ethanol (temperature dependent). The critical S in the figures are somewhat smaller which is due to the fact that the pressure expansion (Fig. 4) goes through a peak supersaturation where nuclei are formed before it comes back to the smaller value. Obviously, when droplets are dispersed about the wire the heat and mass transfer situation is completely upset. This way, the wire experiment is also an indicator of the sudden appearence of droplets by homogeneous nucleation.

For water we have also recorded three curves presented in Fig. 8. Temperatures T_∞ range from 259.1–279.3 K. Much higher excess temperatures and supersaturations are found than in the alcohol cases. Homogeneous nucleation is not reached in accordance with nucleation rate measurements [12] for water. Again the theoretical curves follow the experimental trend in

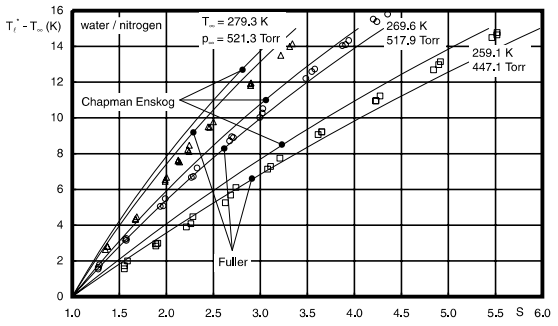

Fig. 8. Experimental results (symbols) and theory (lines) for the excess temperature of the condensing film vs the supersaturation of the ambient vapor for water in nitrogen.

supersaturation, pressure and temperature correctly. The curves for both diffusion coefficients are shown as they differ more than in the alcohol cases. Yet there is no clue as to which model is the better one. A consistent overprediction of the excess temperature appears at the upper curve which may also be observed with the alcohols. A conclusive theoretical or experimental reason for this trend is not available. Investigations at even higher temperatures would be necessary.

5. Conclusions

The present work deals with diffusion controlled vapor condensation in a stagnant gas. Diffusion controlled means that the vapor diffuses through a carrier gas towards the liquid driven by a concentration gradient and that the latent heat diffuses in the opposite direction driven by a temperature gradient. Our focus is on a particular aspect of the problem, namely, the liquid temperature in three basic condensation configurations which are the plane wall, the thin cylinder and the sphere. We show that the liquid temperature takes a steady and equal value in these cases when the ambient state is fixed. From the similarity of the transfer equations, an implicit formula is derived for the calculation of this temperature. It is found to depend on the total pressure, the temperature and the supersaturation of the vapor in the surroundings.

On the experimental side, we present measurements of the liquid temperature of a film condensing onto a thin wire. The measurements take place at the tail of a rapid gas expansion provided by a pex-tube. In the cases of the two alcohols and water carried in nitrogen, the steadiness of the liquid temperature is confirmed. Its value agrees with the theoretical prediction to within a Kelvin. For increasing supersaturation, a limit of diffusion controlled film condensation appears in terms of homogeneously nucleated droplets. The limit correlates with previous nucleation rate measurements.

As our analytical prediction of the liquid temperature is identical for the small cylinder and the small droplet and as the cylinder experiments confirm the analytical result, we have gained indirect confirmation of the temperature of a small droplet at condensation.

Acknowledgements

This work was funded under grant number Pe 401/11 of Deutsche Forschungsgemeinschaft (DFG).

References

[1] J.P.A.J. van Beeck, M.L. Riethmuller, Nonintrusive measurement of temperature and size of single falling raindrops, Appl. Optics 34 (10) (1995) 1633–1639.
[2] L.D. Landau, E.M. Lifschitz, Lehrbuch der Theoretischen Physik VI, Akademie Verlag, Berlin, 1966.
[3] M.N. Özisik, Heat Transfer, McGraw-Hill, New York, 1985.
[4] H. Tautz, Wärmeleitung und Temperaturausgleich, Verlag Chemie, Weinheim, 1971.
[5] J.B. Young, The condensation and evaporation of liquid droplets at arbitrary Knudsen number in the presence of an inert gas, Int. J. Heat Mass Transfer 36 (11) (1993) 2941–2956.
[6] F. Peters, T. Rodemann, Design and performance of a rapid piston expansion device for the investigation of droplet condensation, Exp. Fluids 24 (1998) 300–307.
[7] E.R.G. Eckert, R.M. Drake, Analysis of Heat and Mass Transfer, McGraw-Hill, New York, 1972.
[8] R.C. Reid, J.M. Prausnitz, B.E. Poling, The Properties of Gases and Liquids, McGraw-Hill, New York, 1987.
[9] T. Schmeling, R. Strey, Equilibrium vapor pressure measurements for the *n*-alcohols in the temperature range from −30°C to +30°C, Ber. Bunsenges. Phys. Chem. 87 (1983) 871–874.
[10] D. Sonntag, D. Heinze, Sättigungsdampfdruck und Sättigungs-dampfdichtetafeln für Wasser und Eis, VEB Verlag, Leipzig, 1982.
[11] F. Peters, B. Paikert, Experimental results on the rate of nucleation in supersaturated *n*-propanol, ethanol and methanol vapors, J. Chem. Phys. 91 (9) (1989) 5672–5678.
[12] T. Rodemann, F. Peters, Experimental investigation of binary nucleation rates of water–*n*-propanol and water–*n*-butanol vapors by means of a pex tube, J. Chem. Phys. 105 (12) (1996) 5168–5176.